Space-Charge-Limited Currents Injected from a Point Contact*

M. A. LAMPERT, A. MANY,† AND P. MARK
RCA Laboratories, Princeton, New Jersey
(Received 6 March 1964)

The theory of one-carrier, space-charge-limited currents has been studied for a spherical-flow geometry. The outstanding result is that the initial space-charge-controlled regime in the current-voltage characteristic, following the Ohm's law regime which always obtains at sufficiently low voltages, is universally a $\frac{3}{2}$-power law: $I=KV^{\frac{3}{2}}$. The coefficient K depends on the density and energy distribution of traps, but is independent of both the point-contact radius and the anode radius. This result suggests the possible use of space-charge-limited currents injected from a point as a probe to measure the density of traps locally, i.e., in the neighborhood of the point. Experimental evidence for the $\frac{3}{2}$-power law, obtained with single-crystal CdS, is presented.

I. INTRODUCTION

THERE is an extensive literature[1] dealing with theory and experiments on steady-state, one-carrier space-charge-limited (SCL) injection currents in solids with a planar-flow geometry. In contrast, scant attention has been given to this type of current in other flow geometries, there being only two references[2] in the literature known to the authors. This general lack of interest is, no doubt, explained by the presumed expectation that nothing fundamentally new and interesting would emerge from such a study. It is well known, for example, that for SCL current flow in vacuum, the planar-, spherical-, and cylindrical-flow geometries all yield basically the same I-V (current-voltage) characteristic, namely, $I \propto V^{3/2}$. In fact, it has been demonstrated,[3] via a dimensional analysis, that this same current-voltage relationship obtains for the vacuum problem for electrodes of arbitrary shape.

One of the authors (A.M.) recently had occasion to utilize a point-contact electrode as a means of achieving a high electric-field intensity, locally, in an experimental study of high-field phenomena in conducting cadmium sulfide. In the course of this work it was discovered that when the point was biased negatively, a marked majority-carrier injection was produced (see Fig. 1), even though the thermal-equilibrium density of conduction-band electrons exceeded 10^{15} cm^{-3}. This work, in turn, led to the theoretical study, which is reported here, of steady-state, one-carrier SCL injection currents in a spherical geometry. The point of the report is that our study has brought to light a new result, unique to the spherical geometry, which appears to us of intrinsic interest and, further, which may have important application in the study of defect states in solids.

The outstanding result of our study is as follows: For current injection at a point contact, the initial space-charge controlled regime of the I-V characteristic, following the Ohm's-law regime which always obtains at sufficiently low voltages, is generally of the form: $I=KV^{3/2}$. The constant K depends on the density and energy distribution of the traps in the forbidden gap which can capture and immobilize the injected carriers. However, K is independent of the point-contact radius r_c as well as of the anode radius r_a.

We shall see in the following section that the $\frac{3}{2}$-power law is a consequence of the particular manner in which the injected space charge increasingly spreads into the solid, beyond the immediate vicinity of the injecting contact, as the applied voltage increases. Over the range of voltages for which Ohm's law is valid, the injected space charge is confined essentially inside a radius $r_x<2r_c$. Following the departure from Ohmic behavior, i.e., following the onset of the space-charge-controlled characteristic, the confining radius r_x for the injected space charge increases as $V^{1/2}$, and this relationship leads to the above-cited $\frac{3}{2}$-power law. By the same token it is obvious that only the traps in the neighborhood of the injecting point are initially important for the determination of the coefficient K.

These features of the $\frac{3}{2}$-power law suggest immediately the application of this kind of measurement to the determination of trap densities *locally* in the solid, namely, in the neighborhood of the injecting point contact. It is an important experimental convenience in this measurement that the coefficient K is independent of both the cathode and anode radii. In effect, the measurement itself is then independent of both radii. Thus one need use only a reasonably small point and need not bother to measure its radius. Further, the anode need not be actually spherical; it need be only a broad area contact and can then be quite flat without impairing the measurement. This is particularly convenient in single-crystal studies since a spherical or

* The research reported here was sponsored by the U. S. Army Research Office–Durham, Durham, North Carolina under Contract No. DA-31-124-ARO(D)-84, and by the Air Force Cambridge Research Laboratories, Office of Aerospace Research, U. S. Air Force, Bedford, Massachusetts under Contract No. AF19(604)8353, and by the RCA Laboratories, Princeton, New Jersey.

† Permanent address: Physics Department, Hebrew University, Jerusalem, Israel.

[1] Extensive bibliographies are given in two review papers by M. A. Lampert, Proc. IRE **50**, 1781 (1962); *Reports on Progress in Physics, 1964* (The Institute of Physics and the Physical Society, London, 1964).

[2] L. Patrick, J. Appl. Phys. **28**, 765 (1957), Appendix A; B. Meltzer, J. Electron. Control **8**, 171 (1960).

[3] K. R. Spangenberg, *Vacuum Tubes* (McGraw-Hill Book Company, Inc., New York, 1948), Chap. 8.

hemispherical anode would be a generally impractical configuration.

In Sec. II we discuss the physics underlying the $\frac{3}{2}$-power law and shall derive the law in a rather general way. In Sec. III we establish some useful mathematical results based on limiting functional forms for the field and injected carrier density. In Sec. IV we discuss, in detail, several prototype trapping situations: no traps, deep traps, shallow traps, and an exponential distribution of traps. In Sec. V experimental confirmation of the $\frac{3}{2}$-power law is presented for conducting cadmium sulfide. In Appendix A a rather formal mathematical discussion of the $\frac{3}{2}$-power law is given. In Appendix B the I-V characteristics for two pure space-charge-controlled regimes are given, the corresponding results for cylindrical-flow geometry also being presented.

Throughout the entire discussion it is assumed that $r_c \ll r_a$, since this is the situation of interest. Indeed, it is a necessary condition for existence of the $\frac{3}{2}$-power regime in the I-V characteristic. Under this condition, it is possible to simplify considerably the analytic work through judicious approximations. The resulting simplified treatments have the not inconsiderable virtue of laying bare the underlying physics—a virtue not possessed by the more formal approach of Appendix A.

For the sake of definiteness, we take the one-carrier current to be an electron current. All results are equally valid for hole currents with suitable change of nomenclature. Throughout the article mks units are employed, except where otherwise specified.

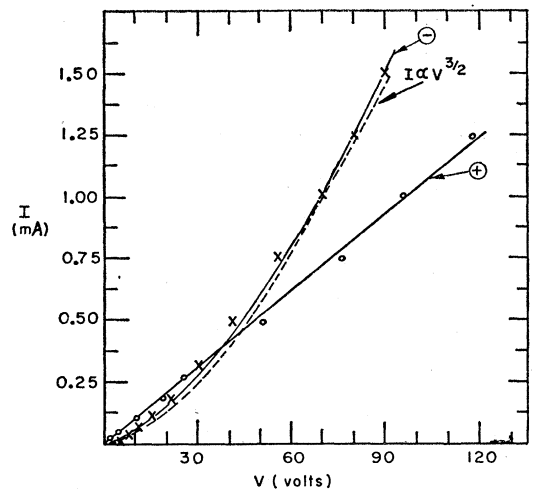

FIG. 1. Current-voltage characteristics obtained with a point-contact electrode on a single crystal of CdS, resistivity 20 Ω-cm. All measurements were made at room temperature. The point radius was $\approx 1\ \mu$. The crosses represent data taken with the point injecting, i.e., biased negatively; the solid line labeled ⊖ is a smooth fit to the data. The dashed curve is a three-halves power-law curve fitted to the data at one point, $I=1$ mA. The open circles represent data taken with the point biased positively. The straight line labeled ⊕ is an Ohm's-law fit to the data.

II. GENERAL DERIVATION OF THE $\frac{3}{2}$-POWER LAW

The equations governing steady-state, one-carrier SCL current flow in spherical geometry are the particle-conservation equation

$$I=4\pi e\mu(n_0+n_i)r^2\mathcal{E}=\text{const}, \tag{1}$$

where, as usual for this type of problem, the diffusive contribution to the current has been neglected; the Poisson equation

$$\epsilon(1/r^2)(d/dr)(r^2\mathcal{E})=e(n_i+n_{t,i}). \tag{2}$$

In the above I is the total current, e the electronic charge, μ the free-electron drift mobility, ϵ the static dielectric constant, $\mathcal{E}$ the electric-field intensity, r the radius, n_0 the thermal-equilibrium free-electron density, n_i the injected, excess free-electron density, and $n_{t,i}$ the injected, excess trapped-electron density.

Further, it is assumed as usual,[4] that the free and trapped carriers in the solid are in quasithermal equilibrium, i.e., that the steady-state Fermi level (SSFL) F, defined by $n_0+n_i=N_c\exp(F-E_c)/kT$, with N_c the effective density of states in the conduction band, E_c the bottom conduction-band level, k Boltzmann's constant, and T the temperature in degrees Kelvin, likewise determines the occupancy of the traps via the Fermi-Dirac occupation function. Finally, we note that the applied voltage

$$V=\int_{r_c}^{r_a}\mathcal{E}dr,$$

with r_c and r_a the cathode and anode radius, respectively.

The boundary condition (B.C.) appropriate to the simplified theory which neglects diffusion is[5]

$$\mathcal{E}=0 \quad \text{at} \quad r=r_c. \tag{3}$$

The above-characterized simplified theory is not, in general, analytically tractable, as is shown in Appendix A. (This is in contrast to the simplified theory for planar flow[5] which is analytically tractable for most cases of interest.) The next step then is further simplification, and the line of procedure is suggested by that portion of the I-V characteristic we wish to examine.

Our interest in this report, whatever the particular problem (trap configuration), is largely confined to the initial space-charge regime of the I-V characteristic, immediately following the Ohm's-law regime. The former is the regime in which the injected space charge is pushing out into the solid beyond the immediate vicinity of the cathode with increasing voltage, but has not yet reached the anode. Let r_x be that radius at which $n_i=n_0$. [Note, from Eq. (2), that $r^2\mathcal{E}$ increases

[4] A. Rose, Phys. Rev. **97**, 1538 (1955).

[5] M. A. Lampert, Phys. Rev. **103**, 1648 (1956).

monotonically with increasing r. Therefore, from (1), n_i decreases monotonically, from ∞ at $r=r_c$, with increasing r. The initial space-charge-controlled regime is, by definition, that regime over which $n_i(r_a)<n_0$.] It is convenient to consider two separate regions of the solid, I and II, and to make the following basic approximations in these regions:

Region I, $r_c\leq r<r_x$: n_0 is neglected;

$$I=4\pi e\mu n_i r^2\mathcal{E}. \quad (4a)$$

Region II, $r_x\leq r\leq r_a$: n_i is neglected;

$$I=4\pi e\mu n_0 r^2\mathcal{E}. \quad (4b)$$

The rationale for these approximations, first introduced by Patrick,[2] rests on the monotonic-decreasing behavior of $n_i(r)$ demonstrated above. The solutions in regions I and II are matched by requiring that the electric field intensity be continuous across r_x.

The total voltage V can, of course, be written as

$$V=V_{c,x}+V_{x,a};\quad V_{c,x}=\int_{r_c}^{r_x}\mathcal{E}dx,\quad V_{x,a}=\int_{r_x}^{r_a}\mathcal{E}dx. \quad (5)$$

Normal, straightforward, analytical development of the solution to the problem as now formulated requires specification of the trap configuration. However, because we wish here to seek out the physical roots of the universal $\frac{3}{2}$-power law, we rest the further analytical development on an essentially dimensional analysis of the properties of the space-charge region I. This analysis effectively skirts the details of the trap configuration. Namely, we assume that the voltage $V_{c,x}$ across region I and the total injected charge

$$Q_x=4\pi e\int_{r_c}^{r_x}(n_i+n_{t,i})r^2dr,$$

contained in region I, can be written, respectively, as

$$V_{c,x}=c_1 r_x\mathcal{E}_x, \quad (6)$$

$$Q_x=c_2(4\pi/3)r_x^3 e(n_0+n_{t,0}), \quad (7)$$

where $\mathcal{E}_x=\mathcal{E}(r_x)$, $n_{t,0}$ is the excess, trapped-electron density in quasithermal equilibrium with the excess free-electron density $n_i=n_0$, and c_1, c_2 are constants of order unity. These assumptions concerning c_1 and c_2 give significant content to the relations (6) and (7).

The relation (6) corresponds to the physical situation in which the main contribution to the voltage $V_{c,x}$ comes from the region of the effective anode for region I, namely at $r=r_x$, rather than from near the cathode. Since $n_i(r_x)=n_0$ and $n_{t,i}(r_x)=n_{t,0}$, the meaning of relation (7) is that the total space charge Q_x in region I is adequately estimated by assuming that the excess charge density at the effective anode, $e(n_0+n_{t,0})$, is uniformly distributed throughout region I. Note that because of the monotonic decreasing character of $n_i(r)$, $c_2\geq 1$ necessarily. A discussion as to why relations (6) and (7) are expected to hold generally is given in Sec. III.

We proceed to the derivation of the $\frac{3}{2}$-power law. First we note that region II is an "Ohmic" region, characterized by

$$V_{x,a}=r_x\mathcal{E}_x;\quad I=4\pi e\mu n_0 r_x V_{x,a}. \quad (8)$$

This is easily shown by noting that in region II, from (1) with $n_i=0$, $\mathcal{E}=A/r^2$ with $A=I/4\pi e\mu n_0$, so that $V_{x,a}=A(r_x^{-1}-r_a^{-1})\simeq A/r_x$, for $r_x\ll r_a$. [Ohm's law for the solid is given by the right-hand I-V relation in (8), taking $r_x=r_c$ and $V_{x,a}=V$.]

From (5), (6), and (8), and from (1) taken at r_x, it follows that

$$r_x\mathcal{E}_x=V/(1+c_1);\quad I=4\pi e\mu n_0 r_x V/(1+c_1). \quad (9)$$

From Gauss' theorem, which is the integral of Eq. (2) from r_c to r_x,

$$r_x^2\mathcal{E}_x=\frac{Q_x}{4\pi\epsilon};\quad r_x=\left\{\frac{3\epsilon V}{(1+c_1)c_2 e(n_0+n_{t,0})}\right\}^{1/2}, \quad (10)$$

where the right-hand relation in (10) follows from the left-hand relation, using (7) and (9).

The final result, the universal $\frac{3}{2}$-power law, follows from substitution for r_x, from (10), into the I-V relation in (9):

$$I=4\pi e\mu n_0\left\{\frac{3\epsilon}{c_2 e(n_0+n_{t,0})}\right\}^{1/2}\left(\frac{V}{1+c_1}\right)^{3/2}. \quad (11)$$

In practical units (11) becomes

$$I=2.6\times 10^{-15}\left\{\frac{\mu^2 n_0^2\kappa}{c_2(n_0+n_{t,0})}\right\}^{1/2}\left(\frac{V}{1+c_1}\right)^{3/2}\text{A}, \quad (11a)$$

with μ in cm^2/V-sec, n_0 and $n_{t,0}$ in cm^{-3}, V in V, and with κ the relative dielectric constant.

Note that Eqs. (11) and (11a) refer to the full spherical geometry. For the hemispherical geometry, used to approximate the point contact, the right-hand sides of Eqs. (11) and (11a) must be divided by two.

In Sec. III it is argued that the possible ranges of c_1 and c_2 are $\frac{1}{2}\leq c_1\leq 2$ and $1\leq c_2\leq 2$, respectively, where the lower limits obtain in the deep-trap situation and the upper limits in the trap-free and shallow-trapping situations. The corresponding variation in the factor $1/c_2^{1/2}(1+c_1)^{3/2}$ in Eqs. (11), (11a) covers the range from $(2/3)^{3/2}=0.545$ at the lower limits to $\frac{1}{3}\sqrt{6}=0.136$ at the upper limits, a factor of four between the two extremes. Explicit values for c_1 and c_2 are calculated for the trap-free, shallow-trap, deep-trap, and exponential distribution trap configurations in Sec. IV.

It remains to determine the onset voltage for the $\frac{3}{2}$-power law regime and the range of voltages over which the law is valid. The onset voltage, i.e., the voltage of transition between Ohm's law and the $\frac{3}{2}$-power law, is

given by the intersection of the I-V law in (8), with $r_x=r_c$ and $V_{x,a}=V$, with the I-V law in (11). Letting subscript "cr" indicate the value of a quantity evaluated at this transition, we readily obtain

$$r_{x,cr}=(1+c_1)r_c; \quad V_{cr}=Q_{x,cr}/4\pi\epsilon r_c;$$
$$I_{cr}=Q_{x,cr}/t_\Omega, \qquad t_\Omega=\epsilon/en_0\mu, \tag{12}$$

where $Q_{x,cr}$ is given by (7) with $r_x=r_{x,cr}$.

By dividing the left-hand relation in (10) by the left-hand relation in (9), we obtain the useful relation:

$$V>V_{cr}: \quad Q=CV, \quad C=4\pi\epsilon r_x/1+c_1. \tag{13}$$

This physically plausible relationship establishes, from the right-hand relation in (10), that $C\propto V^{1/2}$. Note that $C_{cr}=C(V_{cr})=4\pi\epsilon r_c$.

The transition from this initial space-charge-controlled regime of the I-V characteristic to the succeeding regime obviously takes place at that voltage V_{cr}' at which $r_x=r_{x,cr}'\simeq r_a$. Since $r_{x,cr}\simeq r_c$, from (12), it follows from the right-hand relation in (10) that $V_{cr}'/V_{cr}\simeq(r_a/r_c)^2$. Since we have assumed that $r_a\gg r_c$, it follows that the $\frac{3}{2}$-power law obtains over an enormous range of voltages.

All succeeding regimes of the one-carrier SCL I-V characteristic, following the $\frac{3}{2}$-power-law regime, depend explicitly on the anode radius r_a as seen in Table I of Appendix B. Therefore, the theoretical results for these succeeding regimes are applicable only if the physical shape of the anode bears a reasonably close resemblance to a spherical or hemispherical surface. For single-crystal materials these shapes are certainly inconvenient, if not altogether impractical. On the other hand, for the study of polymers or glassy materials, these shapes may indeed prove practical.

From the physical analysis of the $\frac{3}{2}$-power-law regime it follows, since the injected space charge spreads out gradually, with increasing voltage, from the point, that the anode configuration is irrelevant at voltages V such that $r_x\ll(A_a/\pi)^{1/2}$, where A_a is the effective anode area. Further, even if the injecting point contact, of effective area A_c, cannot be adequately represented by a hemispherical electrode, one has the intuitive expectation that the one-dimensional, radial-flow analysis is still applicable to obtain the I-V characteristic over the range of voltages for which $(A_c/\pi)^{1/2}\ll r_x\ll(A_a/\pi)^{1/2}$. Therein lies the potential usefulness of the injecting point as a "probe" to study trapping "locally".

The injecting-point "probe" and the planar-flow measurement technique[1] appear to have rather complementary virtues for the study of defect states in insulators. The former studies traps locally, near the injecting point, and the latter necessarily studies an average over all traps between cathode and anode. The point-contact method is experimentally more convenient in at least two respects. First, where contact difficulties are present, which is frequently the case, they can be more easily overcome with a point contact than with a wide-area contact; e.g., tunnelling to achieve injection is more easily promoted with a small-radius point. Also if injection has to be achieved by electronic means, e.g., electron-bombardment-induced or photoinduced conductivity, a higher density of free carriers can be achieved locally (equivalent point contact). In this connection the use of the naturally narrow-beam laser light may prove exceptionally useful. Thickness requirements with the planar-flow geometry are usually quite severe and often very thin samples have to be used. Certainly, thicker samples can be used with the point-contact technique. On the other hand, for very high-resistivity insulators, e.g., polystyrene, some background, light-stimulated conductivity may be necessary to obtain an n_0 high enough to use the point-contact method conveniently.

In favor of the planar-flow measurements, they can yield both more information, e.g., the trap energy level, from the richer structure in the SCL I-V curve[5] and more accurate information, e.g., a remarkably accurate determination of the average trap density from the trap-filled-limit voltage[5] V_{TFL}. (To be sure, in some cases difficulties of inconsistencies in the derived data have appeared.[6]) The injecting-point measurement at a single temperature yields directly no information about the trap energy level, and further, yields the quantity $n_{t,0}$ in Eq. (11) with a maximum uncertainty of a factor of 16. (Actually, the latter uncertainty can be narrowed by an order of magnitude with only minimal qualitative information about the traps, such as whether they are shallow or deep or distributed in energy. The temperature-dependent behavior of $n_{t,0}$ can be expected to yield such information.)

A further uncertainty relates to our idealization of the injecting-point geometry. We have represented the injecting point mounted against a flat surface by a hemispherical flow geometry and then neglected possible surface effects. If the total number of surface states out to radius r_x are less than Q_x/e, presumably only small errors are introduced by our treatment. However, if these surface states exceed Q_x/e, the magnitude of the error is unknown and remains to be investigated. Here an experimental approach may prove more fruitful, or convenient, than an attempted generalization of the theory.

III. SOME OBSERVATIONS CONCERNING c_1 AND c_2

In this section we note some useful relations concerning c_1 and c_2 and, in particular, give an argument establishing limits on their possible values. We first note two very useful relations

$$\text{If} \quad \mathcal{E}\propto r^n, \quad \text{with} \quad n>-1,$$

then

$$c_1=1/(n+1). \tag{14}$$

[6] R. H. Bube, J. Appl. Phys. 33, 1733 (1962).

If $(n_i+n_{t,i})\propto r^m$ with $0\geq m>-3$,
then

$$c_2=3/(m+3). \tag{15}$$

The exponent m cannot be positive since $n_i+n_{t,i}$ must be nonincreasing with r. These relations are easily proven by substituting the assumed forms for the radial dependence of $\mathcal{E}$ and $(n_i+n_{t,i})$ into the defining integrals for $V_{c,x}$ and Q_x, respectively. The conditions $n>-1$ and $m>-3$ enable us to neglect $r_c{}^{n+1}$ with respect to $r_x{}^{n+1}$, and $r_c{}^{m+3}$ with respect to $r_x{}^{m+3}$, respectively, thereby validating (6) and (7). In analyzing specific problems, as in Sec. IV, the main steps are simply the determination of the exponents n and m.

It remains to verify that indeed $n>-1$ and $m>-3$ always, and further to establish the possible ranges of values for c_1 and c_2, respectively. The basic step in the argument is the representation of the functional relationship between $n_{t,i}$ and n_i by the simple form $n_{t,i}\propto n_i{}^p$. To the extent that such a representation is valid, it is easy to see that $0\leq p\leq 1$. For a given shift of the steady-state Fermi level, $F\rightarrow F+\delta F$, the maximum change in trap occupancy will occur if the traps are shallow, $n_{t,i}\propto n_i$, so that $p=1$, and the minimum change will occur if the traps are deep, i.e., no change at all, $n_{t,i}=\text{const}$, so that $p=0$. More formally, $n_{t,i}\propto n_i{}^p$ is equivalent to $dn_{t,i}/dn_i=pn_{t,i}/n_i$. Now, for a single trap-level the Fermi-Dirac occupancy relationship is

$$n_{t,i}=N_t/[1+(N/gn_i)],\quad N=N_c\exp[(E_t-E_c)/kT],$$

whence

$$dn_{t,i}/dn_i=q(n_{t,i}/n_i),$$

with

$$q=(N/gn_i)/[1+(N/gn_i)],$$

so that $0\leq q\leq 1$ where the left- and right-hand equality signs hold in the respective limits $n_i=\infty$ and $n_i=0$.

Taking $n_{t,i}\gg n_i$ in Eq. (2) (the trap-free case is explicitly calculated in Sec. IV), and noting that $n_{t,i}\propto n_i{}^p\propto(r^2\mathcal{E})^{-p}$ from (4a), Eq. (2) can be written

$$(r^2\mathcal{E})^p d(r^2\mathcal{E})\propto r^2dr,$$

so that

$$(r^2\mathcal{E})^{p+1}\propto r^3.$$

Thus, $\mathcal{E}\propto r^{(1-2p)/(1+p)}$ and $n_i+n_{t,i}\simeq n_{t,i}\propto r^{-3p/(p+1)}$. As p varies from 0 to 1, $(1-2p)/(1+p)$ decreases monotonically from 1 to $-\frac{1}{2}$, and $-3p/(\mathrm{p}+1)$ decreases monotonically from 0 to $-\frac{3}{2}$. Thus, referring to (14) and (15), we see that the $\frac{3}{2}$-power law is indeed validated. Further, the corresponding ranges of c_1 and c_2 are from $\frac{1}{2}$ to 2 and from 1 to 2, respectively.

The above argument is rigorous only to the extent that the representation $n_{t,i}\propto n_i{}^p$ is valid. We have seen above, in discussing a single, discrete set of traps that this representation is indeed valid only in the limit of deep trapping or shallow trapping. For intermediate positions of the Fermi level, the equivalent p is a function of the position, hence of n_i. However since $0\leq p\leq 1$ and since the corresponding ranges of c_1 and c_2, for this range of p, are relatively narrow, it would appear plausible that the $\frac{3}{2}$-power law (11) is indeed generally valid with the coefficients c_1 and c_2 having possibly a very weak voltage dependence, both being bounded within the above-specified relatively narrow limits. The general validity of the $\frac{3}{2}$-power law is argued further in Appendix A.

IV. SOME SPECIFIC TRAP CONFIGURATIONS

We have seen in Sec. II that the $\frac{3}{2}$-power law, Eq. (11), is given in terms of a trap-density parameter $n_{t,0}$ and two dimensionless constants, c_1 and c_2, which depend "weakly" on the trap configuration, being of order unity. The three quantities $n_{t,0}$, c_1, and c_2 are defined in (6) and (7). In this section we discuss briefly four specific trap configurations and compute the relevant quantities for each of them. The four configurations are: A, the trap-free case; B, deep traps; C, shallow traps; and D, an exponential distribution of traps. In every case it is only the region I: $r_c\leq r<r_x$ with which we need be concerned. Here again we shall assume that $r_x\gg r_c$. Where $r_x<3r_c$, we are dealing with the transition from Ohm's law to the $\frac{3}{2}$-power law, and we cannot expect a simplified treatment to describe accurately such transitions.

A. The Trap-Free Case: $n_{t,i}\equiv 0$, $n_{t,0}\equiv 0$

The defining equations are (4a) and (2) with $n_{t,i}=0$. Substituting for n_i from (1) and (2) gives the differential equation $d(r^2\mathcal{E})^2/dr=(I/2\pi\epsilon\mu)r^2$, with solution

$$\mathcal{E}=(I/6\pi\epsilon\mu)^{1/2}[(r^3-r_c{}^3)/r^4]^{1/2}$$
$$\simeq(I/6\pi\epsilon\mu)^{1/2}r^{-1/2},\quad \text{for } r\gg r_c, \tag{16}$$

where the first relationship is the exact one satisfying B.C. (3). Further, since $n_i\propto 1/r^2\mathcal{E}$ from (4a), it follows from the approximate relation for $\mathcal{E}$ in (16) that $n_i\propto r^{-3/2}$. Thus, referring to (14) and (15), $n=-\frac{1}{2}$ and $m=-\frac{3}{2}$, so that $c_1=2$ and $c_2=2$.

The maximum in the $\mathcal{E}$ field, obtained by differentiating the exact form of $\mathcal{E}(r)$ in (16), occurs at $r_m=4^{1/3}r_c\simeq 1.6r_c$ and is given by $\mathcal{E}_m=(1/3\times 2^{1/3})(r_c/r_x)^{1/2}V/r_c$. In view of the presence of the field maximum so close to the cathode, one might well question our use of the approximate form of $\mathcal{E}$ in (16) to evaluate c_1 and c_2 above, since the approximate form is badly in error near the cathode. One way of seeing that the use of the approximate form for $\mathcal{E}$ does not produce significant error is to show that its use in the derivation of the current-voltage characteristic leads to the correct result. Direct integration of (16), taking $\mathcal{E}\propto r^{-1/2}$, gives

$$I=3\pi\epsilon\mu V_{c,x}{}^2/2r_x, \tag{17}$$

which is precisely the result of Meltzer,[2] using the exact form for $\mathcal{E}$ in (16), in the limit $r_x\gg r_c$. Finally we note that the above-derived values for c_1 and c_2 can also

be obtained working directly with (17), rather than with the approximate form of $\mathcal{E}$ in (16).

B. The Deep-Trap Case: $n_{t,i}=p_{t,0}=$ constant

Consider the situation where the only effective traps are a single discrete set lying at an energy E_t below the thermodynamic Fermi level F_0. Let $p_{t,0}$ be the thermal-equilibrium density of unoccupied traps. Where the steady-state Fermi level F has been raised above F_0, through injection, by more than kT, namely over region I, the previously unoccupied traps are filled with electrons and $n_{t,i}\simeq p_{t,0}$. Assuming that $p_{t,0}\gg n_0$, which is the interesting case, it follows that $n_{t,i}>n_i$ over most of region I, namely everywhere except very close to the cathode. It simplifies matters considerably to take $n_{t,i}>n_i$ *everywhere* in region I, so that n_i can then be neglected in Eq. (2), and $n_{t,i}$ is taken equal to $p_{t,0}$. It is then trivial to integrate Eq. (2), obtaining

$$\mathcal{E}=(ep_{t,0}/3\epsilon)[(r^3-r_c^3)/r^2]\simeq(ep_{t,0}/3\epsilon)r\,,\quad \text{for } r\gg r_c, \tag{18}$$

where the first relationship is the exact one satisfying B.C. (3). Further, since $(n_i+n_{t,i})\simeq n_{t,i}=p_{t,0}\propto r^0$, referring to (14) and (15) we see that $n=1$ and $m=0$ so that $c_1=\frac{1}{2}$ and $c_2=1$. To complete the picture, $n_{t,0}=p_{t,0}$.

Here again for this case, one might well raise the question of the magnitude of error introduced by the incorrect treatment of the cathode region. Strictly speaking, the region I should be divided into two separate subregions: region Iα, $r_c\leq r<r_{x'}$, with $n_i(r_{x'})=p_{t,0}$ and region Iβ, $r_{x'}\leq r<r_x$, with $n(r_x)=n_0$ as previously. Over region Iα, $n_i>p_{t,0}$, so that $n_{t,i}$ can be neglected in Eq. (2), and over region Iβ, $n_i<p_{t,0}$, so that n_i can be neglected in Eq. (2). (In the previous argument we have assumed that region Iβ covers all of region I). If this three-region problem is now analyzed one finds, using obvious notation, that

$$V_{x',x}=(V_{c,x'}+V_{x,a})/2\,,$$

so that

$$V=3(V_{c,x'}+V_{x,a})/2.$$

Further, $V_{x,a}/V_{c,x'}=(p_{t,0}/4n_0)^{2/3}$, so that for $p_{t,0}\gg n_0$, $V_{c,x'}$ can be neglected and the above-derived result is shown to be correct.

Since, from (18), $V_{c,x}\simeq ep_{t,0}r_x^2/6\epsilon$, the upper end of the $\frac{3}{2}$-power regime occurs at the voltage $V_{\mathrm{TFL}}\simeq ep_{t,0}r_a^2/6\epsilon$. At this voltage all the traps throughout the volume are filled—hence the subscript TFL, denoting trap-filled-limit. Beyond this point the current rises very steeply with voltage in a manner similar to the planar-flow TFL problem.[5] Details of this regime and its transition to the trap-free regime, Eq. (17), can be readily worked out in terms of the two-region picture, where the two regions are now Iα, $r_c\leq r<r_{x'}$ with $n_i(r_{x'})=p_{t,0}$ as previously, and Iβ, $r_{x'}\leq r\leq r_a$.

Finally, we note that although we have discussed the deep-trap case in terms of one set of traps at a single discrete energy level, it is obvious that the argument holds for an arbitrary distribution of traps provided only that they all lie below F_0 in energy. In this case, $p_{t,0}$ is the total density of unoccupied traps at all energies.

C. The Shallow-Trap Case: $n_i/n_{t,i}=\theta=$ constant

Consider the situation where the only effective traps are a single set of shallow traps, i.e., traps lying at an energy E_t above F_0, of density N_t and statistical weight g. As injection proceeds the steady-state Fermi level F rises in the forbidden gap. So long as $E_t-F>kT$, the ratio of free- to trapped-carrier densities is a constant[4,5] given by $n_i/n_{t,i}=\theta=N/gN_t$, $N=N_c\exp(E_t-E_c)/kT$. This condition will be realized throughout most of region I, except close to the cathode where $F>E_t$ necessarily. For the sake of simplicity assume that this shallow-trap condition holds everywhere in region I. In that case, $n_i+n_{t,i}$ in Eq. (2) can be replaced by n_i/θ, assuming $\theta\ll 1$, which is the interesting case. It is now evident that mathematically the shallow-trap problem is formally identical with the trap-free problem A if ϵ is replaced by $\theta\epsilon$, e.g., in (17), (10), and (11). Since trapping effects are completely subsumed in this substitution, $n_{t,0}$ is taken equal to zero in (7), (10), and (11) and Q_x refers only to free charge. Finally, $c_1=2$ and $c_2=2$, as in the trap-free case, since these quantities are unaffected by the above substitution.

If one wants to treat the cathode region more rigorously, it is necessary to divide region I into three separate subregions: Region Iα, $r_c\leq r<r_{x''}$, with $n_i(r_{x''})=N_t$; region Iβ, $r_{x''}\leq r<r_{x'}$, with $n_i(r_{x'})=\theta N_t$; and region Iγ, $r_{x'}\leq r<r_x$, with $n(r_x)=n_0$. In region Iα, $n_{t,i}$ is neglected in Eq. (2); in region Iβ, n_i is neglected and $n_{t,i}=N_t=$ constant; and in region Iγ, n_i is neglected and $n_{t,i}=n_i/\theta$. With $r_x\gg r_c$, the corrections introduced by this more rigorous treatment are indeed small and the above-derived result holds as stated. This more careful treatment of region I is, however, useful for the study of succeeding regimes in the space-charge-controlled current-voltage characteristic, a matter which we do not pursue further here.

D. An Exponential Distribution of Traps

In materials which have a high density of different kinds of localized defect states, either of chemical or structural origin, it is not unreasonable to expect that the different trap states can be well represented by a continuous distribution in energy. A particularly convenient distribution for theoretical analysis is the exponential distribution,[4] which further has proven very useful in the interpretation of experimental data on space-charge-limited currents.[4,7] Such a distribution can be represented in the form $N_t(E)=N_0\exp(E-E_c)/$

[7] For example, P. Mark and W. Helfrich, J. Appl. Phys. **33**, 205 (1962); H. P. D. Lanyon, Phys. Rev. **130**, 134 (1963).

kT_c, where $N_t(E)$ is the trap density per unit energy range and T_c is a convenient temperature parameter characterizing the trap distribution. The integrated trap density $n_t(F)$ between the thermodynamic Fermi level F_0 and the steady-state Fermi level F is approximately $n_t(F)\simeq kT_cN_0\exp(F-E_c)/kT_c$, where we have assumed that $\exp(F-F_0)/kT_c\gg 1$. Now, *so long as* $l=T_c/T>1$, $n_t(F)$ is also, to a good approximation, the density of trapped electrons corresponding to position F. (For $l<1$, the uppermost trap states, energetically, dominate the trapping of injected carriers and the entire situation is simply a shallow-trap one, already discussed.) Since $n=N_c\exp(F-E_c)/kT$, which is the defining equation for F, the relation between free and trapped charge is $n_{t,i}=kT_cN_0(n_i/N_c)^{1/l}$, with $l>1$. Referring to Sec. III, we see that $\mathcal{E}\alpha r^n$ with $n=(l-2)/(l+1)$ and $n_{t,i}\propto r^m$, with $m=-3/(l+1)$. Referring now to (14) and (15), we see that indeed the $\frac{3}{2}$-power law is valid with $c_1=(l+1)/(2l-1)$ and $c_2=(l+1)/l$.

V. EXPERIMENTAL VERIFICATIONS OF THE $\frac{3}{2}$-POWER LAW

In Fig. 1 is shown the measured current-voltage characteristic for injection from a point contact of radius $r_c\approx 1\mu$ into a single crystal of CdS at room temperature. It is seen that $I\propto V^{3/2}$ gives a good fit to the data. (With the polarity such that the point is positive, Ohm's law is observed over the entire voltage range, as expected.) Since the room-temperature resistivity ρ of the sample was 20 Ω-cm, the corresponding trap-free $\frac{3}{2}$-power law, Eq. (11a) with $c_1=2$, $c_2=2$, and $n_{t,0}=0$, is $I=4.77\times V^{3/2}\times 10^{-6}$ A, for V in V, taking $\epsilon/\epsilon_0=9.3$ and $\mu=200$ cm²/V-sec, and dividing by two to take the hemispherical geometry into account. The experimental curve in Fig. 1 is fitted by $I=1.75\times V^{3/2}\times 10^{-6}$ A. From (11) it can then be concluded that trapping is taking place with $n_{t,0}/n_0\simeq 7$. Since $\rho=20$ Ω-cm corresponds to $n_0\simeq 10^{15}$ cm^{-3}, the thermodynamic Fermi level F_0 was $\simeq 0.2$ eV below the conduction band. The observation of trapping effects in this circumstance is not unexpected for CdS.

The above experiment, although indeed confirming the $\frac{3}{2}$-power law, is rather fragmentary in nature since it was designed for an entirely different purpose, namely for the study of high-field effects in CdS, and was carried out in advance of the above theoretical developments. We may anticipate in the future a much more comprehensive study of the $\frac{3}{2}$-power law, involving points of different radii and carried out over a substantial temperature range.

ACKNOWLEDGMENTS

The authors would like to thank Alfred Willis for his assistance in carrying out the experiment described in Sec. V, and the Computation Laboratory of the RCA Laboratories for its assistance in carrying out the digital computation needed to obtain the exact coefficient for the $\frac{3}{2}$-power law for the trap-free problem quoted in Appendix A.

APPENDIX A: FURTHER MATHEMATICAL DISCUSSION

In formulating the general problem in spherical geometry it is convenient to rewrite Eqs. (1) and (2) as follows:

$$I=4\pi e\mu nr^2\mathcal{E}=\text{const}, \tag{A1}$$

$$\frac{\epsilon}{e}\frac{1}{r^2}\frac{d}{dr}(r^2\mathcal{E})=(n-n_0)+\sum_j(n_{t,j}-n_{t,j,0}), \tag{A2}$$

where n is the total free-carrier density; $n=n_0+n_i$, $n_{t,j}$ is the density of electrons in the jth set of traps of density $N_{t,j}$, statistical weight g_j, and located at energy level $E_{t,j}$; and $n_{t,j,0}$ is the value of $n_{t,j}$ in thermal equilibrium (no applied voltage). Where there is a distribution of traps continuous in energy, $\sum_j$ is to be replaced by an integration, $\int dE$.

The quasithermal equilibrium relationship between the $n_{t,j}$ and n is expressed by the Fermi-Dirac occupation function, written in the form

$$\begin{aligned} n_{t,j}&=\frac{N_{t,j}}{1+(N_j/g_jn)},\\ p_{t,j}&=N_{t,j}-n_{t,j}=\frac{N_jN_{t,j}/g_jn}{1+(N_j/g_jn)},\\ N_j&=N_c\exp\frac{E_{t,j}-E_c}{kT}. \end{aligned} \tag{A3}$$

It is useful to define dimensionless variables as follows:

$$\begin{aligned} &u=n_0/n, && i=3\epsilon I/4\pi e^2n_0^2\mu r_c^3,\\ &v=12\pi en_0\mu r_cV/I, && z=(r/r_c)^3. \end{aligned} \tag{A4}$$

In terms of these variables, Eqs. (A1) and (A2) combine to give the equation

$$\begin{aligned} i\frac{du}{dz}&=\frac{1-u}{u}+\sum_j B_j\frac{1-u}{1+C_ju};\\ C_j&=\frac{N_j}{g_jn_0},\quad B_j=\frac{N_{t,j}}{n_0}\frac{C_j}{(1+C_j)}, \end{aligned} \tag{A5}$$

and the voltage relationship

$$V=\int_{r_c}^{r_a}\mathcal{E}dr$$

becomes

$$v=\int_1^{z_a}\frac{udz}{z^{4/3}},\quad z_a=\left(\frac{r_a}{r_c}\right)^3. \tag{A6}$$

It is obvious that the integration in (A6) cannot be

performed analytically, even for the simplest case, namely with all $B_j=0$ in (A5), i.e., the case of no traps.

For further discussion it is convenient to consider first a few simple cases:

I. The Trap-Free Case

Since there are no traps, all of the $B_j\equiv 0$, so that (A5) can be written

$$udu/(1-u)=\{-1+1/(1-u)\}du=(1/i)dz\,, \quad \text{(A7)}$$

with solution

$$-u-\ln(1-u)=(1/i)(z-1)=w\,, \quad \text{(A8)}$$

satisfying B.C. (3). In terms of the variable w, (A6) becomes

$$v=i^{-1/3}\int_0^{w_a}\frac{udw}{(w+1/i)^{4/3}}\,, \quad w_a=\frac{1}{i}(z_a-1)\simeq\frac{z_a}{i}\,. \quad \text{(A9)}$$

The range of the variable u is $0\leq u<1$. From (A8) it follows that for $w>6$, $0.999<u<1$. Thus, for $z>1+6i$ or $w>6$ there is negligible error in taking $u=1$ in (A6) and (A9).

Ohm's-Law Regime

Rewrite (A6) as $v=I_1+I_2$ with

$$I_1=\int_1^{1+6i}udz/z^{4/3}$$

and

$$I_2=\int_{1+6i}^{z_a}dz/z^{4/3}=3\{(1+6i)^{-1/3}-z_a^{-1/3}\}\,.$$

Now, for $i\ll 1/6$, $I_1<6i\ll 1$ and $I_2\simeq 3$. Thus $v\simeq 3$, which corresponds, from (A4), to Ohm's law: $I=4\pi en_0\mu r_c V$.

$\frac{3}{2}$-Power Regime

Consider currents i in the range $1\ll i\ll z_a$. There will be an enormous range of currents satisfying these inequalities even for r_a/r_c as small as 100, since then $z_a=10^6$. Rewrite (A9) as $v=i^{-1/3}K$, $K=K_1+K_2$ with

$$K_1=\int_0^6 udw\Big/\left(w+\frac{1}{i}\right)^{4/3}$$

and

$$K_2=\int_6^{w_a}dw\Big/\left(w+\frac{1}{i}\right)^{4/3}$$

$$=3\left\{\left(6+\frac{1}{i}\right)^{-1/3}-\left(w_a+\frac{1}{i}\right)^{-1/3}\right\}.$$

For the range of i's considered, $K_2\simeq 3/6^{1/3}$ and

$$K_1\simeq\int_0^6 udw/w^{4/3}=8.84\,,$$

as determined with the aid of a digital computer. Thus $v=10.49i^{-1/3}$, or from (A4),

$$I=1.06\pi en_0\mu(\epsilon/en_0)^{1/2}V^{3/2}. \quad \text{(A10)}$$

The approximate result (11), taking $n_{t,0}=0$ and $c_1=c_2=2$ as determined in Sec. IV, is the same as (A10) except that the numeric 1.06 is replaced by $4/3\sqrt{2}=0.94$.

In the above discussion, the approximation of K_1 by

$$\int_0^6 udw/w^{4/3}$$

involves a small error (an overestimate) in the range, approximately, $0\leq w\leq 1/i$. The integral

$$\int_0^{1/i}udw\Big/\left(w+\frac{1}{i}\right)^{4/3}\approx(1/i)^{-4/3}\int_0^{1/i}udw$$

$$\simeq(2\sqrt{2}/3)(1/i)^{1/6}\,,$$

since for small w, $u\simeq(2w)^{1/2}$ from (A8). In the above we have used

$$\int_0^{1/i}udw/w^{4/3}\simeq 6\sqrt{2}(1/i)^{1/6}.$$

Thus, for $1/i$ small enough, the error is negligible.

II. The Deep-Trap Case

Consider a single set of traps lying below F_0 so that $C=N/gn\ll 1$ in (A3) and (A5), where we have suppressed the subscript j. Thus the single-trap term on the right-hand-side of Eq. (A5) is $B(1-u)/(1+Cu)\simeq B(1-u)$. With this approximation, (A5) can be written as

$$[1/(1-u)-1/(1+Bu)]du=[(1+B)/i]dz=dw\,, \quad \text{(A11)}$$

with solution

$$-\ln(1-u)-(1/B)\ln(1+Bu)$$

$$=[(1+B)/i](z-1)=w. \quad \text{(A12)}$$

The voltage integral (A6) can now be written as

$$v=\left(\frac{i}{1+B}\right)^{-1/3}\int_0^{w_a}\frac{udw}{[w+(1+B)/i]^{4/3}}\,, \quad w_a\simeq\frac{1+B}{i}z_a\,. \quad \text{(A13)}$$

The $\frac{3}{2}$-power law corresponds to the current range $1\ll i/(1+A)\ll z_a$. Following the same procedure as in the preceding case I, we write (A13) as

$$v=[i/(1+B)]^{-1/3}K\,, \quad K=K_1+K_2$$

with

$$K_1=\int_0^6 udw\Big/\left\{w+\frac{1+B}{i}\right\}^{4/3}$$

and

$$K_2=\int_6^{w_a} dw \Big/ \left\{w+\frac{1+B}{i}\right\}^{4/3}$$
$$=3\left\{\left(6+\frac{1+B}{i}\right)^{-1/3}-\left(w_a+\frac{1+B}{i}\right)^{-1/3}\right\}.$$

For the range of i's considered,

$$K_2\simeq 3/6^{1/3}=1.65 \quad \text{and} \quad K_1\simeq\int_0^6 udw/w^{4/3}.$$

As with case I, K_1 can only be evaluated, using (A11) or (A12) with the aid of a computer, which has not been done.

Noting that for deep traps, $C\ll 1$, the quantity $B\simeq p_{t,0}/n_0$ with $p_{t,0}=N_t-n_{t,0}$, the final result can be written, assuming $p_{t,0}\gg n_0$ or $B\gg 1$, as

$$I=(9/K^{3/2})4\pi e n_0\mu(\epsilon/e p_{t,0})^{1/2}V^{3/2}, \qquad \text{(A14)}$$

where K remains to be evaluated. The approximate result (11), taking $n_{t,0}=p_{t,0}\gg n_0$ and $c_1=\frac{1}{2}$, $c_2=1$, as determined in Sec. IV, is the same as (A14) except that the quantity $9/K^{3/2}$ is replaced by $2^{3/2}/3=0.94$.

As with case I above, the approximation of K_1 by

$$\int_0^6 udw/w^{4/3}$$

is in error over the range $0\leq w\leq(1+B)/i$. However, it is easily shown that

$$\int_0^{(1+B)/i} udw/w^{4/3}$$

is in any case negligibly small for $(1+B)/i\ll 1$.

III. The General Case

This case is characterized by Eq. (A5). An analysis along the same lines as followed in cases I and II above gives the result

$$v=\left(\frac{i}{1+B}\right)^{-1/3}\int_0^{w_a}\frac{udw}{[w+(1+B)/i]^{4/3}},$$
$$B=\sum_j\frac{B_j}{1+C_j}, \quad w_a=\frac{1+B}{i}z_a. \qquad \text{(A15)}$$

Again, in the current range

$$1\ll\frac{i}{1+B}\ll z_a, \quad v=[i/(1+B)]^{-1/3}K,$$

with

$$K=K_1+K_2, \quad K_1\simeq\int_0^6 udw/w^{4/3}$$

and

$$K_2\simeq 3/6^{1/3},$$

where K_1 can only be evaluated with the aid of a computer; and again the $\frac{3}{2}$-power law is obtained.

APPENDIX B: A COMPARISON OF TWO PURE SPACE-CHARGE REGIMES IN THREE GEOMETRIES

In the accompanying Table I we present the calculated current-voltage characteristics for two situations, the trap-free crystal and the crystal with an exponential distribution of traps, neglecting the thermal free carriers n_0, in three different one-dimensional flow geometries:

TABLE I. I-V characteristics for pure space-charge regimes (n_0 negligible). I corresponds to current injection at r_c, collection at r_a; I_r corresponds to the reverse polarity.

Current-flow geometry	No traps[d]	Exponential distribution of traps: $N_t(E)=N_0\exp(E-E_c)/kT_c$; $l=\frac{T_c}{T}>1$
Plane-parallel[a]	$I=\frac{9}{8}\epsilon\mu A\frac{V^2}{(r_a-r_c)^3}$	$I=\left[\frac{\epsilon l}{eN_0kT_c(l+1)}\right]^l(e\mu N_cA)\left[\frac{2l+1}{l+1}\right]^{l+1}\frac{V^{l+1}}{(r_a-r_c)^{2l+1}}$
Cylindrical[b]	$I=2\pi\epsilon\mu L\frac{V^2}{r_a^2}$	$I=\left[\frac{2\epsilon l}{eN_0kT_c(l+1)}\right]^l(2\pi e\mu N_cL)\left[\frac{2l}{l+1}\right]^{l+1}\frac{V^{l+1}}{r_a^{2l}}$
	$I_r=I\left[\ln\left(\frac{r_a}{r_c}\right)\right]^{-2}$	$I_r=I\left[\frac{2l}{l+1}\ln\left(\frac{r_a}{r_c}\right)\right]^{-(l+1)}$
Spherical[c]	$I=\frac{3\pi}{2}\epsilon\mu\frac{V^2}{r_a}$	$I=\left[\frac{3\epsilon l}{eN_0kT_c(l+1)}\right]^l(4\pi\epsilon\mu N_c)\left[\frac{2l-1}{l+1}\right]^{l+1}\frac{V^{l+1}}{r_a^{2l-1}}$
	$I_r=I\left[\frac{r_a}{2r_c}\right]^{-2}$	$I_r=I\left[\frac{2l-1}{l+1}\frac{r_a}{r_c}\right]^{-(l+1)}$

[a] A is the electrode area; (r_a-r_c) is the cathode-anode spacing; $I_r\equiv I$.
[b] L is the length of the cylinder; it is assumed that $r_a\gg r_c$.
[c] It is assumed that $r_a\gg r_c$.
[d] The shallow-trap result is given simply by multiplying the corresponding expressions by θ, the ratio of free to trapped charge.

the planar, cylindrical, and spherical geometries. As noted in Table I, the result for the shallow-trap situation is obtained from the trap-free situation simply by inclusion of the θ factor, which is just the ratio of free to shallow-trapped charge. As noted in the text, for the spherical geometry the pure space-charge I-V characteristics depend explicitly on the outer radius r_a. It is seen that a like result holds also for the cylindrical geometry. The functional dependence of I on V is seen to be the same, for any trap configuration, in all three flow geometries—a result reminiscent of the $I \propto V^{3/2}$ for the vacuum diode independent of flow geometry.[3] For the sake of completeness the characteristics i_r with reversed polarity of applied voltage are also presented. These latter characteristics are presented in a manner which gives directly the rectification ratio i_r/i. It is seen that this rectification ratio for spherical geometry can be very small indeed, and is much smaller than the corresponding ratio for cylindrical flow for the same r_a/r_c.

PHYSICAL REVIEW VOLUME 135, NUMBER 5A 31 AUGUST 1964

Artificial Metals: InSb, the Sn Alloys with InSb, and Metallic InTe†

A. J. DARNELL AND W. F. LIBBY
Department of Chemistry and Institute of Geophysics, University of California, Los Angeles, California
(Received 9 April 1964)

The metallic forms of indium antimonide, indium telluride, and the metallic alloys InSbSn, $InSbSn_2$, and $InSbSn_4$, were prepared at high temperature and high pressure, cooked, and subsequently quenched to −197°C before release of the pressure to one atmosphere. The metastable metallic forms can be retained at one atmosphere pressure at low temperatures indefinitely and studied conveniently. InSb(II) and its metastable alloys with tin have lattice parameters essentially identical with those of metallic tin. The lattice parameter of the cubic form of indium telluride is 6.177±0.002 Å at 25°C. The compressibilities of InSb(II), InSb(I) and of Sn(β) at −197°C are 0.9, 3.6, and 3.1×10^{-6} bar^{-1}, respectively. The compressibilities of InTe(I) and InTe(II) at 25°C are 6.3 and 3.8×10^{-6} bar^{-1}, respectively. The heat of transformation ΔH^0_{210}, (1 atm) InSb(II) → InSb(I) is −4.77±0.04 kcal per mole. The resistivity of InSb(II) at 77°K is 77×10^{-6} Ω-cm. The velocity of sound in polycrystalline InSb(II) is approximately 3900 m/sec. The Brinnel hardness numbers of InSb(II) and Sn(β) at 77°K are 230 and 46 kg mm^{-1}. InTe(II) is diamagnetic, its susceptibility is −0.14 emu g^{-1}.

I. INTRODUCTION

IT has been demonstrated experimentally[1–7] by Kennedy and his co-workers, by Drickamer and his co-workers, and by others that diamond-type lattices, when subjected to pressure, suffer a transformation into a denser, more highly coordinated state, which is metallic. The general nature of the phase diagram is that the melting point of the nonmetallic state falls as the pressure is increased until a triple point is reached and the solid-solid transition corresponding to a change from a nonmetallic to a metallic state occurs after which the melting point rises again with an increase in pressure. It is thought that this general phase diagram applies for all the members of group IV; carbon, silicon, germanium, etc., and to the binary compounds one column removed from group IV in the periodic table such as boron nitride, aluminum phosphide, gallium arsenide, indium antimonide, etc., and even those two removed from group IV (though less work has been done on them) such as zinc selenide, which averages four valence electrons per atom.

It is our purpose here to describe a technique of removing these new materials from the high-pressure apparatus in which they were produced in order that their properties can be studied more completely. The difficulties and limitations of having to work within a high pressure chamber are very great.

II. THE TECHNIQUE

It is very well known in chemistry that a transition from one solid phase to another or from a liquid to a solid or, in some instances, in the opposite direction can be slow and dependent upon nuclei. The transformation of metallic tin to the semiconducting, diamond-type structure at low temperatures well illustrates this.

† This research was supported by the Directorate of Chemical Sciences, United States Air Force Office of Scientific Research, Grant No. AF-AFOSR-245-64.

[1] A. Jayaraman, R. C. Newton, and G. C. Kennedy, Nature **191**, 1288 (1961).
[2] A. Jayaraman, W. Klement, Jr., and G. C. Kennedy, Phys. Rev. **130**, 540 (1963).
[3] B. J. Alder and R. H. Christian, Phys. Rev. Letters **8**, 367 (1961).
[4] H. L. Suchan and H. G. Drickamer, J. Chem. Phys. **31**, 355 (1959).
[5] S. Minomura and H. G. Drickamer, Phys. Chem. Solids **23**, 451 (1962).
[6] G. A. Samara and H. G. Drickamer, Phys. Chem. Solids **23**, 457 (1962).
[7] G. A. Samara and H. G. Drickamer, J. Chem. Phys. **37**, 408 (1962).